J|A|C|S
ARTICLES

Published on Web 10/27/2009

Hyperpolarized [2-^{13}C]-Fructose: A Hemiketal DNP Substrate for In Vivo Metabolic Imaging

Kayvan R. Keshari,[†,‡] David M. Wilson,[†] Albert P. Chen,[§] Robert Bok,[†] Peder E. Z. Larson,[†] Simon Hu,[†] Mark Van Criekinge,[†] Jeffrey M. Macdonald,[‡] Daniel B. Vigneron,[†] and John Kurhanewicz*[,†]

Department of Radiology and Biomedical Imaging, University of California San Francisco (UCSF), 1700 fourth St., Byers Hall 203, San Francisco, California 94158; Department of Biomedical Engineering, University of North Carolina—Chapel Hill (UNC), 152 MacNider Hall, Campus Box 7575, Chapel Hill, North Carolina, 27599; and GE Healthcare, 333 Ravenswood Ave., Building 207, Menlo Park, California 94025

Received June 16, 2009; E-mail: John.Kurhanewicz@radiology.ucsf.edu

Abstract: Hyperpolarized ^{13}C labeled molecular probes have been used to investigate metabolic pathways of interest as well as facilitate *in vivo* spectroscopic imaging by taking advantage of the dramatic signal enhancement provided by DNP. Due to the limited lifetime of the hyperpolarized nucleus, with signal decay dependent on T_1 relaxation, carboxylate carbons have been the primary targets for development of hyperpolarized metabolic probes. The use of these carbon nuclei makes it difficult to investigate upstream glycolytic processes, which have been related to both cancer metabolism as well as other metabolic abnormalities, such as fatty liver disease and diabetes. Glucose carbons have very short T_1s (<1 s) and therefore cannot be used as an *in vivo* hyperpolarized metabolic probe of glycolysis. However, the pentose analogue fructose can also enter glycolysis through its phosphorylation by hexokinase and yield complementary information. The C_2 of fructose is a hemiketal that has a relatively longer relaxation time (≈16 s at 37 °C) and high solution state polarization (≈12%). Hyperpolarized [2-^{13}C]-fructose was also injected into a transgenic model of prostate cancer (TRAMP) and demonstrated difference in uptake and metabolism in regions of tumor relative to surrounding tissue. Thus, this study demonstrates the first hyperpolarization of a carbohydrate carbon with a sufficient T_1 and solution state polarization for *ex vivo* spectroscopy and *in vivo* spectroscopic imaging studies.

Introduction

Recent development of techniques to retain highly polarized spins in solution via dynamic nuclear polarization (DNP) has enabled hyperpolarized ^{13}C NMR spectroscopy and MR spectroscopic imaging studies with signal enhancements of over 10 000 fold in short acquisition times.[1,2] This new technique has powerful applications for metabolic imaging of cancer. The in vivo metabolism of [1-^{13}C]-pyruvate and its metabolic products, [1-^{13}C]-lactate, [1-^{13}C]-alanine, and [^{13}C] bicarbonate, have been shown to correlate with disease progression[3] and response to therapy[4] in animal models. DNP substrates require a long T_1 relaxation to facilitate efficient spin diffusion during the process of hyperpolarization.[5,6] Carbonyl carbons, which lack attached protons and limit the relaxation as a result of dipolar cross relaxation, have been the standard species to label and polarize with T_1's on the order of 40−60 s, depending on the field strength.[7−9]

Although a number of molecules of interest have been polarized and observed through their carbonyl carbons,[1,3,9−11] a great number of important metabolic intermediates do not contain a carbonyl. Specifically, changes in carbohydrate metabolism occur with the evolution and progression of cancer[12−14] as well as a number of other human diseases such

[†] University of California San Francisco.
[‡] University of North Carolina—Chapel Hill.
[§] GE Healthcare.

(1) Ardenkjaer-Larsen, J. H.; Fridlund, B.; Gram, A.; Hansson, G.; Hansson, L.; Lerche, M. H.; Servin, R.; Thaning, M.; Golman, K. *Proc. Natl. Acad. Sci. U. S. A.* **2003**, *100*, 10158–10163.
(2) Golman, K.; Zandt, R. I.; Lerche, M. H.; Pehrson, R.; Ardenkjaer-Larsen, J. H. *Cancer Res.* **2006**, *66*, 10855–10860.
(3) Albers, M. J.; Bok, R.; Chen, A. P.; Cunningham, C. H.; Zierhut, M. L.; Zhang, V. Y.; Kohler, S. J.; Tropp, J.; Hurd, R. E.; Yen, Y. F.; Nelson, S. J.; Vigneron, D. B.; Kurhanewicz, J. *Cancer Res.* **2008**, *68*, 8607–8615.
(4) Day, S. E.; Kettunen, M. I.; Gallagher, F. A.; Hu, D. E.; Lerche, M.; Wolber, J.; Golman, K.; Ardenkjaer-Larsen, J. H.; Brindle, K. M. *Nat. Med.* **2007**, *13*, 1382–1387.
(5) Abragam, A.; Goldman, M. *Rep. Prog. Phys.* **1978**, *41*, 395–463.
(6) Borghini, M. *Phys. Rev. Lett.* **1968**, *20*, 419–421.
(7) Chen, A. P.; Kurhanewicz, J.; Bok, R.; Xu, D.; Joun, D.; Zhang, V.; Nelson, S. J.; Hurd, R. E.; Vigneron, D. B. *Magn. Reson. Imaging* **2008**, *26*, 721–726.
(8) Merritt, M. E.; Harrison, C.; Storey, C.; Jeffrey, F. M.; Sherry, A. D.; Malloy, C. R. *Proc. Natl. Acad. Sci. U. S. A.* **2007**, *104*, 19773–19777.
(9) Wilson, D. M.; Hurd, R. E.; Keshari, K. R.; Van Criekinge, M.; Chen, A. P.; Nelson, S. J.; Vigneron, D. B.; Kurhanewicz, J. *Proc. Natl. Acad. Sci. U. S. A.* **2009**, *106*, 5503–5507.
(10) Schroeder, M. A.; Atherton, H. J.; Ball, D. R.; Cole, M. A.; Heather, L. C.; Griffin, J. L.; Clarke, K.; Radda, G. K.; Tyler, D. J. *FASEB J.* **2009**, *23*, 2529–2538.
(11) Warren, W. S.; Jenista, E.; Branca, R. T.; Chen, X. *Science* **2009**, *323*, 1711–1714.
(12) Denko, N. C. *Nat. Rev. Cancer* **2008**, *8*, 705–713.

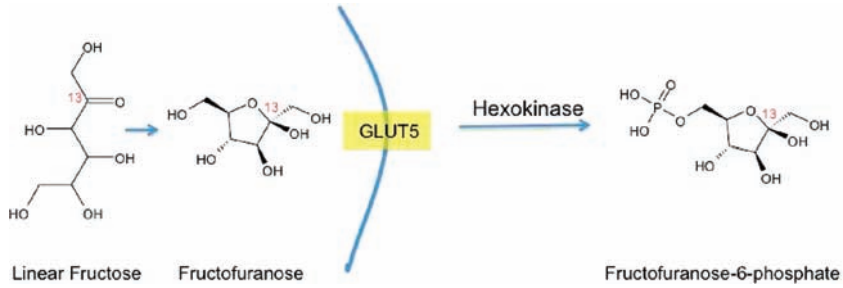

Figure 1. The mechanism for transport by GLUT5 and the first step of metabolism of fructose to fructofuranose-6-phosphate by hexokinase.

as nonalcoholic fatty liver disease.[15−17] Glucose carbons have very short T_1's (<1 s) and therefore uniformly ^{13}C labeled glucose, a mainstay of current metabolic studies,[18,19] cannot be used as an in vivo hyperpolarized metabolic probe of glycolysis.

Fructose, occurring as an isomeric mixture of five- and six-membered rings, has as its most stable isomer β-fructopyranose with a hemiketal in the C_2 position. Fructose can enter glycolyis via hexokinase or fructokinase.[20−24] The one-step metabolism via hexokinase to the phosphorylated fructose-6-phosphate is analogous to the first step of glycolysis, in which glucose is phosphorylated to glucose-6-phosphate. The metabolic flux to fructose-6-phosphate in the cell is related to the downstream glycolytic metabolic events as well as activity of the pentose phosphate pathway (PPP).[25−27] The pentose phosphate pathway is responsible for the predominant amount of nucleotide synthesis (which is increased at high turnover rates) and has been postulated to be a source of regeneration of NADPH in cancer cells,[14] making them more resistant to oxidative stress and allowing them to replenish glutathione.

Furthermore, metabolism of fructose is implicated in nonalcoholic steatohepatitis (NASH),[15] and in the pathogenesis of specific types of cancer. Fructose can also be metabolized to the fructose-1-phosphate via fructokinase, a reaction that takes place primarily in the liver.[20] Hepatic uptake is via the GLUT5 transporter, that demonstrates relative specificity for fructose. Expression of this transporter may be an important biomarker for disease in extrahepatic tissues. For example, the human fructose transporter, GLUT5 (as shown in Figure 1), is highly expressed in breast cancer cell lines but not by normal breast tissue.[28] A recent study of metabolites in the prostate gland has also shown a relationship between fructose and benign versus cancer tissues.[29] Thus, the goal of this study was to investigate a new noncarbonyl hyperpolarized ^{13}C probe, [2-^{13}C]-fructose for the study of metabolism in vivo.

Materials and Methods

Hyperpolarized [2-^{13}C]-Fructose. A 4.0 M solution of [2-^{13}C]-fructose (Isotec, Miamisburg, OH) in water containing 15 mM OX063 trityl radical (Oxford Instruments) was hyperpolarized on a Hypersense instrument (Oxford Instruments) as previously described.[1] The frozen sample was dissolved in 1× phosphate buffered saline (PBS), with a resultant pH of 7.6, and transferred immediately to a 10 mm NMR tube.

11.7T NMR Studies. NMR studies were performed on an 11.7T Varian INOVA spectrometer (125 MHz ^{13}C, Varian Instruments) using a 10 mm $^{15}N/^{31}P/^{13}C$ broadband direct detect probe and temperature controlled at 37 °C. Initially, a thermal spectrum was acquired for a natural abundance fructose sample in 1× PBS buffer at 37 °C (nt = 9000, sw = 30 000, np = 30 000, T_R = 3.5 s, acq time = 0.5s) using a 45° pulse. Figure 2 demonstrates the natural abundance ^{13}C spectrum of fructose. The C_2 carbon resonances are denoted by the blue brackets and correspond to the isomeric distribution of the two ring forms (pyranose and furanose forms) of the fructose molecule. For the acquisition of hyperpolarized ^{13}C spectra eighty pulse and acquire hyperpolarized ^{13}C NMR spectra (1 scan, spectral window = 20 000 Hz, number of points = 40 000, T_R = 3 s, total acquisition time = 2 min 55s) were acquired using a 5° pulse and proton decoupled using a waltz-16 decoupling scheme. Hyperpolarized studies were followed by acquisition of thermal data with nearly identical parameters, using a 90° flip angle and a repetition time of greater than four T_1's (T_R = 300 s, nt = 16). For T_1 measurements hyperpolarized solution was placed into an NMR tube preheated to 37 °C, and this temperature is maintained using the variable temperature unit of the NMR spectrometer. T_1's were determined by collecting a series of spectra with 3 s temporal resolution, starting 12 s after dissolution. These spectra were then fit to a monoexponential function to determine the spin−lattice relaxation time as previously described.[9,30,31] Percent polarization in solution was calculated by comparing the first hyperpolarized spectrum acquired with its thermal spectrum, correcting for differences in tip angle (5 versus 90), and the number of transients (1 versus 16) obtained. Solution state polarizations were calculated by correcting the enhancement for the T_1 relaxation during the

(13) Ganapathy, V.; Thangaraju, M.; Prasad, P. D. *Pharmacol. Ther.* **2008**, *121*, 29–40.
(14) Kroemer, G.; Pouyssegur, J. *Cancer Cell* **2008**, *13*, 472–482.
(15) Farrell, G.; Larter, C. *Hepatology* **2006**, *43*, S99–S112.
(16) Huynh, M.; Luiken, J. J.; Coumans, W.; Bell, R. *Obesity (Silver Spring)* **2008**, *16*, 1755–1762.
(17) Douard, V.; Ferraris, R. P. *Am. J. Physiol. Endocrinol. Metab.* **2008**, *295*, E227−237.
(18) Antoniewicz, M. R.; Kelleher, J. K.; Stephanopoulos, G. *Metab. Eng.* **2006**, *8*, 324–337.
(19) Lane, A. N.; Fan, T. W.; Higashi, R. M.; Tan, J.; Bousamra, M.; Miller, D. M. *Exp. Mol. Pathol.* **2009**, *86*, 165–173.
(20) Bais, R.; James, H. M.; Rofe, A. M.; Conyers, R. A. *Biochem. J.* **1985**, *230*, 53–60.
(21) Skoog, M.; Johansson, G.; Olsson, B.; Appelqvist, R. *Mikrochim. Acta* **1988**, *III*, 131–142.
(22) Funari, V.; Herrera, V.; Freeman, D.; Tolan, D. *Mol. Brain Res.* **2005**, *142*, 115–122.
(23) Petersen, A.; Kappler, F.; Szwergold, B. S.; Brown, T. R. *Biochem. J.* **1992**, *284* (Pt 2), 363–366.
(24) Levi, J.; Cheng, Z.; Gheysens, O.; Patel, M.; Chan, C. T.; Wang, Y.; Namavari, M.; Gambhir, S. S. *Bioconjugate Chem.* **2007**, *18*, 628–634.
(25) Voet, D.; Voet, J. G. *Biochemistry*; 3rd ed.; John Wiley & Sons: New York, 2004.
(26) Tong, X.; Zhao, F.; Thompson, C. B. *Curr. Opin. Genet. Dev.* **2009**, *19*, 32–37.
(27) Vizán, P.; Alcarraz-Vizán, G.; Díaz-Moralli, S.; Solovjeva, O.; Frederiks, W.; Cascante, M. *Int. J. Cancer* **2009**, *124*, 2789–2796.
(28) Zamora-León, S. P.; Golde, D. W.; Concha, I. I.; Rivas, C. I.; Delgado-López, F.; Baselga, J.; Nualart, F.; Vera, J. C. *Proc. Natl. Acad. Sci. U. S. A.* **1996**, *93*, 1847–1852.
(29) Sreekumar, A.; et al. *Nature* **2009**, *457*, 910–914.
(30) Gallagher, F. A.; Kettunen, M. I.; Day, S. E.; Lerche, M.; Brindle, K. M. *Magn. Reson. Med.* **2008**, *60*, 253–257.
(31) Golman, K.; Ardenkjaer-Larsen, J. H.; Petersson, J. S.; Mansson, S.; Leunbach, I. *Proc. Natl. Acad. Sci. U. S. A.* **2003**, *100*, 10435–10439.

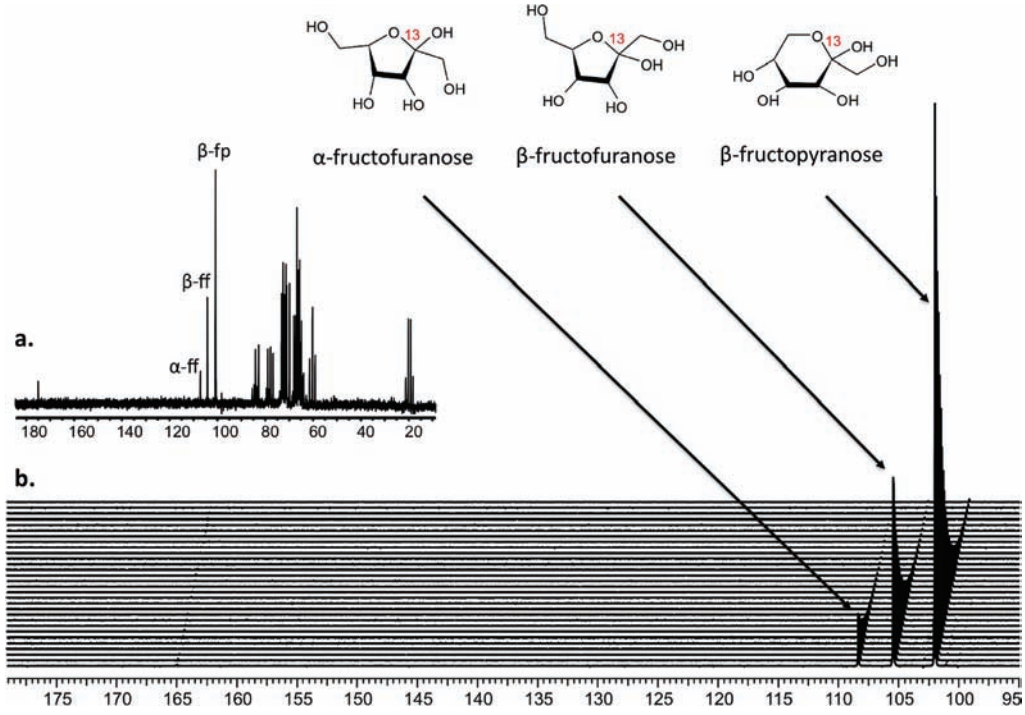

Figure 2. The natural abundance spectrum of fructose (a) and DNP spectrum of [2-^{13}C]-fructose (b). The linear form is present in the DNP spectrum, but at a very low level analogous to the thermal spectrum. (Top) Structures of each of the isomers are shown with their analogous resonance.

transfer time (12 s) from the polarizer to the spectrometer, and the thermal polarization at 11.7T (9.6 ppm).

For NMR studies of the enzymatic conversion of fructose to fructose-6-phosphate, hyperpolarized [2-^{13}C]-fructose was reacted with 400 U of hexokinase (Sigma Aldrich) in the presence of 15 mM ATP, 50 mM TRIS, and 13 mM $MgCl_2$. The labeling and mechanism for transport and metabolism is shown below (Figure 1), though in this enzymatic study the transport element has been removed and the enzyme activity was independently measured. Peaks corresponding to fructose-6-phosphate were identified using a natural abundance carbon spectrum, using a similar set of experimental parameters.

3T Studies. T_1 studies were performed using a 3T GE Signa scanner (GE Healthcare, Waukesha, WI) equipped with the MNS (multinuclear spectroscopy) hardware package similar to studies at 11.7T, with temperature maintained using a heating pad calibrated to 37 °C. Solution spectra were acquired using a 5° nonlocalized pulse, $T_R = 3$ s and fit to a monoexponential. The RF coil used in these experiments was a dual-tuned ^{1}H−^{13}C coil with a quadrature ^{13}C channel and linear ^{1}H channel construction based on an earlier design and also used in ^{13}C-pyruvate mouse imaging studies. For animal studies, T_2-weighted fast spin echo images were acquired prior to MRSI studies to denote anatomy and place voxels on the region of interest. In vivo MRSI studies were carried out using a compressed sensing double spin 3D MRSI acquisition scheme as previously published[32] with a $T_E = 140$ ms, $T_R = 215$ ms, FOV = 8 × 8 cm, and 16 × 8 resolution. 500 μL of of 80 mM [2-^{13}C]-fructose (0.0013 mmol/kg) was injected similar to previously described methods for [1-^{13}C] pyruvate in a transgenic model of prostate cancer (TRAMP).[3] High dose infusions of fructose (0.5 g/kg) can lead to hyperuricemia,[33] but this is well above the dose given in these studies (0.24 mg/kg). These injections were compared to the standard [1-^{13}C]-pyruvate injection for the same voxel in a tumor region of interest. Maps of resonance distributions were generated from the peak heights in each voxel and overlaid on the corresponding T_2-weighted image.

Table 1. T_1 Relaxation Times at 11.7T and 3T and Percent Polarization for Each Fructose Isomer[a]

isomer	T_1sec (11.7T)	T_1sec (3T)	%pol
β-fructopyranose	16.3 ± 0.5	14.5 ± 0.3	12.0 ± 2.2
β-fructofuranose	15.8 ± 0.5	13.4 ± 0.5	11.6 ± 2.5
α-fructofuranose	15.8 ± 0.5	13.4 ± 0.4	11.8 ± 2.0

[a] T_1 relaxation time at 11.7T and 3T ($N = 3$ for both, ± s.d.) are shown for each of the isomers as well as percent polarization ($N = 3$), which have been corrected for the time from dissolution to measurement. All studies were conducted at 37°C.

Results and Discussion

Calculated T_1's for the C_2 fructose carbon are tabulated in Table 1 for the cyclic isomers of fructose (β-fructofuranose, β-fructopyranose, α-fructofuranose) at both 11.7T and 3T, the field stenghts of the ex vivo and in vivo hyperpolarized studies. The open chain (linear) isomer of fructose is present in very small amounts (0.4%)[21,34] and not observed in the hyperpolarized NMR spectra. There was no significant difference in the C_2 T_1 between the cyclic isomers of fructose, most likely due to the fast chemical of the isomeric forms.[34] There was a small decrease in T_1 relaxation (~2 s) of the C_2 carbon with decreasing magnetic field strength from 11.7T to 3T (Table 1). To date, hyperpolarized ^{13}C agents have involved labeling at carbonyl positions, such as the C_1 position of pyruvate, due to their relatively long T_1's.[1,2,7,9,30,35] In contrast to the quaternary hemiketal carbon of the fructose isomers, carbonyl carbons decrease in T_1 with increasing field strengths.[36] This difference is predominantly due to chemical shift anisotropy dominating

(32) Hu, S.; Lustig, M.; Chen, A. P.; Crane, J.; Kerr, A.; Kelley, D. A.; Hurd, R.; Kurhanewicz, J.; Nelson, S. J.; Pauly, J. M.; Vigneron, D. B. *J. Magn. Reson.* **2008**, *192*, 258–264.
(33) Wang, Y. M.; van Eys, J. *Annu. Rev. Nutr.* **1981**, *1*, 437–475.
(34) Goux, W. J. *J. Am. Chem. Soc.* **1985**, *107*, 4320–4327.
(35) Gallagher, F. A.; Kettunen, M. I.; Day, S. E.; Hu, D. E.; Ardenkjaer-Larsen, J. H.; in't Zandt, R.; Jensen, P. R.; Karlsson, M.; Golman, K.; Lerche, M. H.; Brindle, K. M. *Nature* **2008**, *453*, 940–U973.

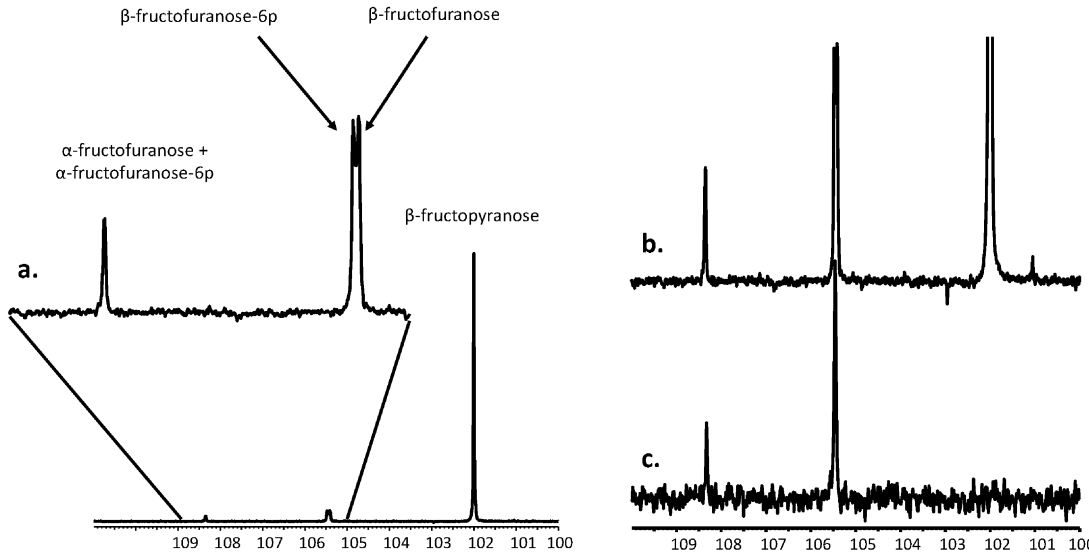

Figure 3. (a) Spectrum of fructose reacted with 400 U of hexokinase, the zoomed in region demonstrates the resonances corresponding to the fructose and fructose-6-phosphate. (b) The dynamic spectrum after 5 s of reaction with hexokinase. (c) The thermal spectrum of same solution with hexokinase averaged 85 min post DNP.

the T_1 relaxation of carbonyl carbons at higher field strengths.[36] This does not hold for the hemiketal of fructose, leading to the typical lengthening of T_1 with increasing field strength. Percent polarizations (Table 1) show similar values for the isomers of fructose with an average solution state polarization at 37 °C of 12%. These polarization values are comparable, although somewhat lower, than those reported for other compounds of interest[1,37,38] such as pyruvate which has been reported to be polarized from 21−30%.[3,39] There was no T_1 dependence on pH observed for pH ranges 5.9−7.8 for the fructose isomers.

The polarization levels were calculated relative to thermal signals from the same sample. The DNP polarizer sits in the fringe field of the 11.7T spectrometer in order to eliminate the possibility of passing the hyperpolarized sample through a zero field and loosing all polarization. For carbonyls such as the C_1 of pyruvate, we know that the T_1 increases at lower magnetic

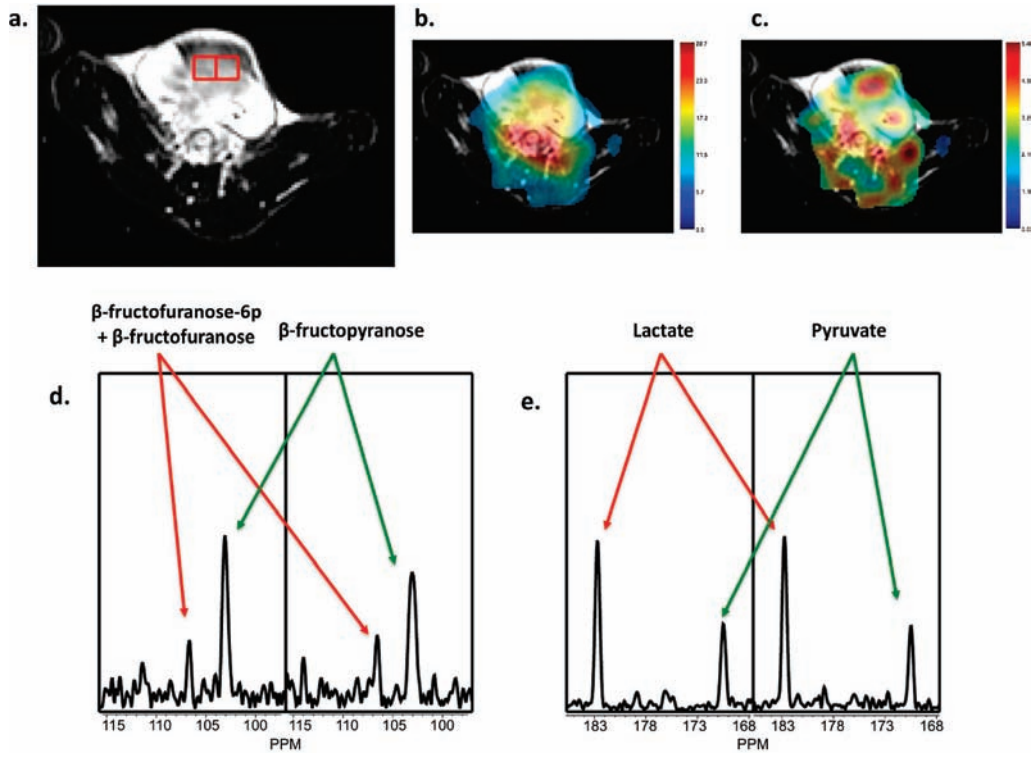

Figure 4. (a) T_2-weighted image of a moderate to late stage TRAMP mouse prostate tumor. Metabolite image overlays of the resonances corresponding to total hyperpolarized fructose (b) and composite β-fructofuranose-6-phosphate and β-fructofuranose (c) obtained after injection of 80 mM [2-^{13}C] fructose demonstrate spatial differences in total fructose versus the composite β-fructofuranose-6-phosphate resonance. Spectra corresponding to the two red voxels (d) in the tumor demonstrate the resonances corresponding to β-fructopyranose and the composite β-fructofuranose-6-phosphate and β-fructofuranose. Pyruvate and lactate resonances are shown from the same locations (e) obtained after an injection of 80 mM hyperpolarized pyruvate in the same mouse.

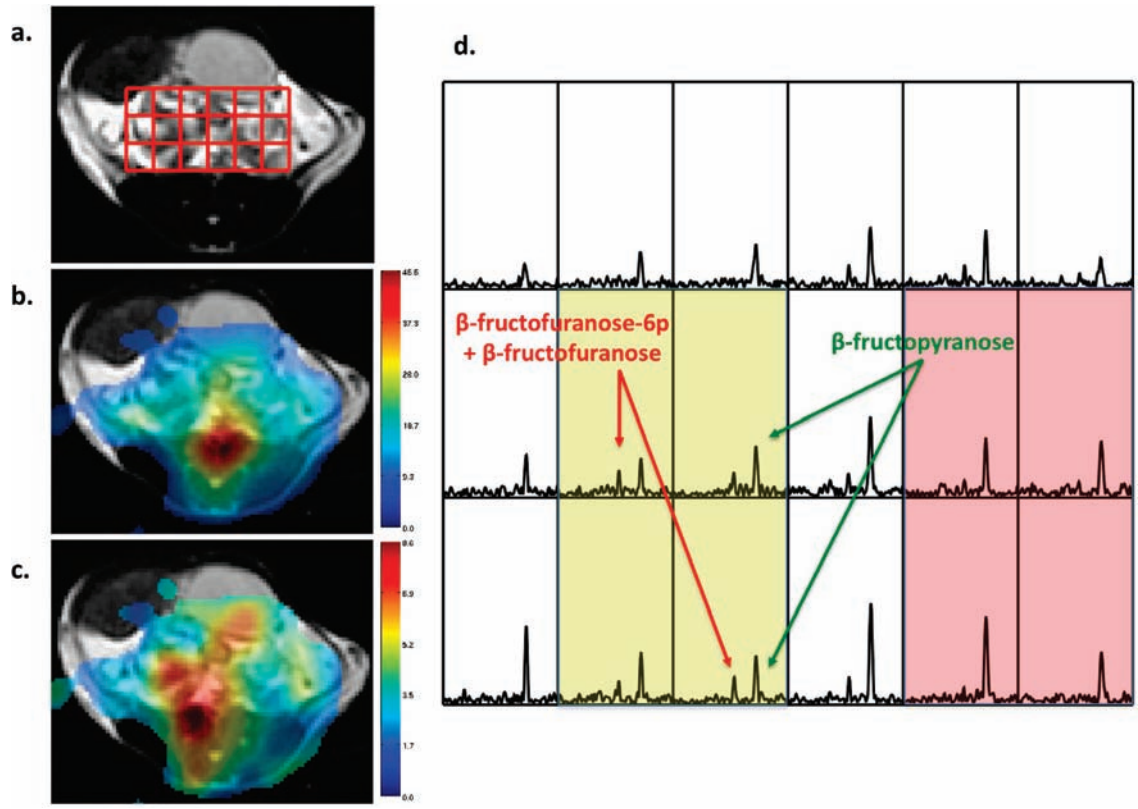

Figure 5. (a) T_2-weighted image of a TRAMP mouse with tumor only on the right side of the prostate. Metabolic images of total hyperpolarized [2-^{13}C] fructose resonances (b) and the composite β-fructofuranose-6-phosphate and β-fructofuranose (c) are shown overlaid on the T_2 weighted image. Resonances corresponding to the β-fructopyranose and composite β-fructofuranose-6-phosphate and β-fructofuranose are shown in the corresponding spectral array (d). The yellow area demonstrates a region of tumor, compared to a region of benign prostate tissue in red. An unassigned spurious, low signal-to-noise resonance appears at 115 ppm.

field strengths, and that the T_1 in the fringe field of the magnet should be longer, on the order of 80 s as compared to 52 s at 11.7T. This is due to the relationship between CSA and field strength (CSA $\propto B_0^2$), which dominates the carbonyl T_1 at high field strengths.[36] However, as demonstrated in this publication, the T_1 of the quaternary C_2 carbon of fructose is only slightly longer at higher field strengths (Table 1). Therefore, the T_1 in the fringe field should be slightly shorter than 3T, which would result in a small underestimation of the % polarization at time zero.

The reaction of hyperpolarized C_2-fructose with hexokinase after addition of fructose to the hexokinase in buffer within the NMR yields the phosphorylated pentose within 5 s (Figure 3). An expansion of the downfield region of the spectrum (Figure 3a) shows the split in the 105.5 ppm resonance, which is a combination of both the β-fructofuranose and the β-fructofuranose-6-phosphate (the predominant isomeric form of fructose-6-phosphate). Figure 3 also compares the first scan of the hyperpolarized acquisition (Figure 3b) versus the thermal spectrum acquired over 85 min post DNP (Figure 3c). It is apparent that the enzyme has now fully converted the fructose to fructose-6-phosphate and there is no longer a resonance corresponding to β-fructopyranose.

Figure 4 demonstrates the metabolism following separate injections of 80 mM hyperpolarized fructose (Figure 4d) and pyruvate (Figure 4e) in the same TRAMP mouse. As previously published,3 the primary TRAMP tumor demonstrates high levels of hyperpolarized lactate, as well good signal-to-noise spectra of hyperpolarized fructose and it is metabolite β-fructofuranose-6-phosphate. Injections of 80 mM hyperpolarized fructose yielded an average total signal-to-noise ratio of 21.0 $\pm$ 2.1 in tumor slices (an average of 70 voxels in 2 slices was used for $N = 3$ TRAMP mice). Because the isomeric ratio of the fructose pyranose to furanose in solution is $\sim$77/23[21] the in vivo peak at 105.5 ppm (and if visible the downstream 108.25 ppm resonance) is not solely due to β-fructofuranose-6-phosphate but also has a small contribution from β-fructofuranose. In this relatively large TRAMP tumor, both high levels of LDH activity and hexokinase activity were observed 15 s postinjection in the same 0.035 cm^3 voxels. Figure 4b demonstrates the distribution of the total fructose signal throughout the slice, a measure of combined delivery and uptake of hyperpolarized Fructose. Slightly higher levels of total hyperpolarized fructose were observed in the tumor region relative to surrounding muscle in the same slice. In comparison, Figure 4c demonstrates the distribution of the resonance at 105.5 ppm, which includes the metabolite β-fructofuranose-6-phosphate. Importantly, this resonance has a good signal-to-noise ($\sim$5:1) and is colocalized in regions of high lactate within the tumor (Figure 4, parts d and e).

(36) Ven, F. J. M. v. d. *Multidimensional NMR in Liquids: Basic Principles and Experimental Methods*; Wiley-VCH: New York, 1995; pp 356–358.
(37) Merritt, M. E.; Harrison, C.; Storey, C.; Sherry, A. D.; Malloy, C. R. *Magn. Reson. Med.* **2008**, *60*, 1029–1036.
(38) Kohler, S. J.; Yen, Y.; Wolber, J.; Chen, A. P.; Albers, M. J.; Bok, R.; Zhang, V.; Tropp, J.; Nelson, S. J.; Vigneron, D. B.; Kurhanewicz, J.; Hurd, R. E. *Magn. Reson. Med.* **2007**, *58*, 65–69.
(39) Schroeder, M. A.; Cochlin, L. E.; Heather, L. C.; Clarke, K.; Radda, G. K.; Tyler, D. J.; Shulman, R. G. *Proc. Natl. Acad. Sci. U. S. A.* **2008**, *105*, 12051–12056.

Figure 5 demonstrates a case where there was tumor only in the left side of the murine prostate, providing a direct comparison of hyperpolarized fructose uptake/delivery and metabolism between benign and malignant prostate tissues. The MRSI data demonstrated that the resonance corresponding to the composite β-fructofuranose and β-fructofuranose-6-phosphate were higher in the regions of tumor as compared to the benign prostate tissues (Figure 5d). Interestingly, there is no difference in total hyperpolarized fructose in regions of malignant versus benign prostate tissue. However, the composite β-fructofuranose and β-fructofuranose-6-phosphate resonance (Figure 5c) was higher in malignant left lobe of the prostate as compared to the benign right side (Figure 5, parts c and d).

Conclusions

In this study, [2-^{13}C]-fructose was hyperpolarized using the DNP method and shown to have sufficiently long T_1's and polarizations sufficient for hyperpolarized ^{13}C NMR spectroscopic and MRSI studies. The hemiketal C_2 of fructose demonstrates the first noncarbonyl to be hyperpolarized for use as a metabolic probe and suggests the potential of using other hyperpolarized probes involving quaternary carbons even those in ring structure. Enzymatic conversion of hyperpolarized [2-^{13}C]-fructose, to fructose-6-phosphate has been demonstrated in vitro and in vivo. While the composite β-fructofuranose and β-fructofuranose-6-phosphate resonance was associated with tumor regions, it was also present in some surrounding benign tissues, and additional studies are necessary to fully understand the composition of this resonance and its relationship to malignancy. The enzymatic conversion of hyperpolarized fructose allows the probing of important changes in glycolytic metabolism upstream of pyruvate, including upregulated hexose uptake,[28] hexokinase activity, and changes in flux through the pentose phosphate pathway.[14] Although, this study was focused on prostate cancer models, upstream glyolytic processes have been the basis of a number of cancer studies including the HIF-1 and PI3K related processes.[14] Therefore, changes in fructose metabolism may be important in the assessment of therapies that target these pathways. A potential link between fructose metabolism and nonalcoholic fatty liver disease has also been demonstrated,[40] and thus hyperpolarized fructose could become a valuable metabolic imaging agent to study this and other diseases both ex vivo and in vivo. Moreover, the dose of fructose given in this murine study translates into a very safe patient dose.

Acknowledgment. The authors would like to acknowledge the following funding mechanisms for supporting this research: National Institutes of Health (R21 EB005363, R01 EB007588, and R21 GM075941) and NIBIB T32 Training Grant 1 T32 ED001631.

Supporting Information Available: The complete citation of ref 29 is available as well as the full CSI data spectral matrix for the studies corresponding to Figures 4 (Figure S1) and 5 (Figure S2). This material is available free of charge via the Internet at http://pubs.acs.org.

JA9049355

(40) Donnelly, K. L.; Smith, C. I.; Schwarzenberg, S. J.; Jessurun, J.; Boldt, M. D.; Parks, E. J. *J. Clin. Invest.* **2005**, *115*, 1343–1351.